Received: 16 January 2024 | Revised: 12 April 2024 | Accepted: 14 May 2024

DOI: 10.1002/jbma.37755

RESEARCH ARTICLE

Society For Biomaterials WILEY

Development and characterization of antacid microcapsules to buffer the acidic intervertebral disc microenvironment

Jennifer Gansau[1,2,3] | Emily E. McDonnell[1,2] | Conor T. Buckley[1,2,4,5]

[1]Trinity Centre for Biomedical Engineering, Trinity Biomedical Sciences Institute, Trinity College Dublin, The University of Dublin, Dublin, Ireland

[2]Discipline of Mechanical, Manufacturing and Biomedical Engineering, School of Engineering, Trinity College Dublin, The University of Dublin, Dublin, Ireland

[3]Department of Orthopaedics, Icahn School of Medicine at Mount Sinai, New York, USA

[4]Advanced Materials and Bioengineering Research (AMBER) Centre, Royal College of Surgeons in Ireland & Trinity College Dublin, The University of Dublin, Dublin, Ireland

[5]Tissue Engineering Research Group, Department of Anatomy and Regenerative Medicine, Royal College of Surgeons in Ireland, Dublin, Ireland

Correspondence
Conor T. Buckley, Trinity Centre for Biomedical Engineering, Trinity Biomedical Sciences Institute, Trinity College Dublin, Ireland.
Email: conor.buckley@tcd.ie

Funding information
Science Foundation Ireland: Career Development Award, Grant/Award Number: 15/CDA/3476

Abstract

During intervertebral disc (IVD) degeneration, microenvironmental challenges such as decreasing levels of glucose, oxygen, and pH play crucial roles in cell survival and matrix turnover. Antacids, such as $Mg(OH)_2$ and $CaCO_3$, entrapped in microcapsules are capable of neutralizing acidic microenvironments in a controlled fashion and therefore may offer the potential to improve the acidic niche of the degenerated IVD and enhance cell-based regeneration strategies. The objectives of this work were, first, to develop and characterize antacid microcapsules and assess their neutralization capacity in an acidic microenvironment and, second, to combine antacid microcapsules with cellular microcapsules in a hybrid gel system to investigate their neutralization effect as a potential therapeutic in a disc explant model. To achieve this, we screened five different pH- neutralizing agents ($Al(OH)_3$, $Mg(OH)_2$, $CaCO_3$, and HEPES) in terms of their pH neutralization capacities, with $Mg(OH)_2$ or $CaCO_3$ being carried forward for further investigation. Antacid-alginate microcapsules were formed at different concentrations using the electrohydrodynamic spraying process and assessed in terms of size, buffering kinetics, cell compatibility, and cytotoxicity. Finally, the combination of cellular microcapsules and antacid capsules was examined in a bovine disc explant model under physiological degenerative conditions. Overall, $CaCO_3$ was found to be superior in terms of neutralization capacities, release kinetics, and cellular response. Specifically, $CaCO_3$ elevated the acidic pH to neutral levels and is estimated to be maintained for several weeks based on Ca^{2+} release. Using a disc explant model, it was demonstrated that $CaCO_3$ microcapsules were capable of increasing the local pH within the core of a hybrid cellular gel system. This work highlights the potential of antacid microcapsules to positively alter the challenging acidic microenvironment conditions typically observed in degenerative disc disease, which may be used in conjunction with cell therapies to augment regeneration.

KEYWORDS
buffer, $CaCO_3$, $Mg(OH)_2$, nucleus pulposus, pH

1 | INTRODUCTION

Cell-based therapies for intervertebral disc (IVD) regeneration may hold significant potential to rejuvenate disc tissue and provide a long-term solution for low back pain. However, the degenerated disc is characterized by a harsh microenvironment with low levels of oxygen (5%–10%), glucose (1–5 mM), and high levels of lactic acid (2–6 mM).[1–3] In particular, the acidic pH evolving due to lactate accumulation and impaired metabolite diffusion during disc degeneration plays a crucial role for cell survival and matrix turnover.[4] This is critical, not only for resident disc cells, but also for any of the cell types proposed for tissue regeneration. Many researchers have investigated the use of nucleus pulposus (NP) cells for regenerating the IVD, which have been shown to delay degenerative disc changes after reimplantation in animal models.[5,6] However, several limitations are associated with using culture expanded autologous NP cells, including poor cell yield after isolation, limited 2D expansion capacities and risk of tissue damage at the harvest site during cell isolation.[7–9] Therefore, alternative cell types including articular chondrocytes (ACs) have been proposed for NP regeneration.[10,11] As fully differentiated primary cells, ACs exhibit some phenotypical differences to NP cells. However, they are easily accessible and capable of matrix deposition similar to NP tissue, which makes them attractive candidates to be considered for IVD repair.

Within a healthy IVD, the average pH has been reported to be 7.1.[3,12] With the onset of degeneration, the pH within the NP decreases to approximately 6.7–6.9 and can decrease further to 6.5 in a severely degenerated IVD.[3,13] Wuertz et al. demonstrated that matrix acidity has detrimental effects on bone marrow stem cells (BMSCs) inhibiting cell proliferation, diminished cell viability, and inhibited anabolic gene expression.[14] This has also been observed for disc-chondrocytes cultured in nutrient-deprived conditions at a pH of 6.2[15] with the accumulation of sulfated glycosaminoglycans (sGAG), a key component of disc tissue, found to be inhibited below a pH of 6.8.[16,17] In our previous work when investigating pH effects on cells cultured in 3D hydrogels, we also observed increased death and diminished matrix accumulation in lower pH microenvironments for both alginate encapsulated BMSCs[18] and NP cells cultured in extracellular matrix (ECM) hydrogels.[19]

A potential strategy to overcome this challenge is to precondition or prime cells using growth factors.[20–23] Our laboratory and others have demonstrated that inducing BMSCs toward a discogenic phenotype using the growth factor TGF-β improves matrix deposition and enhances cell viability in a disc-like microenvironment.[24,25] We have also made similar findings using ACs, which deposited similar levels of sGAG and collagen compared to BMSCs in acidic conditions after 2 weeks of priming using TGF-β3, and exhibited greater viability compared with BMSCs at a pH of 6.5.[22] Nevertheless, the harsh nutrient microenvironment of low oxygen, glucose, and pH remains, affecting resident cells and inhibiting the regeneration process. Acidity appears to be one of the main challenges, whereby it reduces viability and matrix anabolism. Therefore, a possible solution is to increase the local pH of the tissue toward neutral levels, which may improve cellular function and aid in the enhancement of ECM deposition.

Antacids are multicomponent salts with pH neutralizing properties and have been widely used to treat symptoms such as heartburn and dyspepsia, which are associated with hyper-acidic gastric fluids.[26] They are a group of salts whose active component is often based on aluminum hydroxide ($Al(OH)_3$), magnesium hydroxide ($Mg(OH)_2$), sodium bicarbonate ($NaHCO_3$), calcium carbonate ($CaCO_3$), or combinations thereof. $CaCO_3$ has previously been used for its acid-sensitive properties in drug release vehicles for the manipulation of cancer microenvironments.[27,28] Specifically, a drug is encapsulated into a core of $CaCO_3$, which dissolves within the acidic carcinogenic environment and releases its content. For instance, Zhao et al. fabricated a vehicle of amorphous calcium carbonate/doxorubicin@Silica, which released doxorubicin in mildly acidic conditions (pH 6.5), resulting in efficient cell death of cancer cells.[29] HEPES (4-(2-hydroxyethyl)-1-piperazineethanesulfonic acid), a zwitterionic sulfonic agent also has acidic buffering capacities and is commonly used to supplement cell culture media to maintain its pH within a neutral range (pH 6.8–8.2). Microencapsulation of pH neutralizing salts has been shown to improve the release kinetics for prolonged functionality.[30] For example, Chen et al. encapsulated $Mg(OH)_2$ into alginate spheres to investigate release kinetic patterns depending on sphere size and alginate concentration. They demonstrated a correlation of higher $Mg(OH)_2$ release in smaller alginate spheres as well as lower alginate concentration, indicating the ability to fine-tune the antacid delivery in low pH environments.[30] In terms of hydrogels, fibrin has been widely employed in clinical settings as a sealant and adhesive. Previous work in our laboratory demonstrated that the incorporation of hyaluronic acid (HA) can increase the bioactivity of fibrin-based hydrogels resulting in enhanced sGAG accumulation by ACs.[31] Therefore, a combination of antacid microcapsules with a fibrin-based gel may provide promise for minimally invasive disc repair.

The overall objective of this work was to develop and characterize pH neutralizing microcapsules and investigate their potential to buffer the typical acidic conditions that exist in vivo. Specifically, different antacids ($Al(OH)_3$, $Mg(OH)_2$, $CaCO_3$, or HEPES) were initially compared in terms of their pH neutralization capacities, with $Mg(OH)_2$ or $CaCO_3$ being carried forward for further investigation and characterization. Specifically, we examined the impact of microcapsules containing $Mg(OH)_2$ or $CaCO_3$ antacids on both cell viability and matrix accumulation in vitro and in an ex vivo disc explant model under physiological degenerative-like conditions.

2 | MATERIALS AND METHODS

2.1 | Experimental design

An overview of the experimental design is illustrated in Figure 1. Overall, this study was divided into three phases. In the first phase, different types of buffering salts and agents ($Al(OH)_3$, $Mg(OH)_2$, $CaCO_3$, and HEPES) were assessed in terms of their pH neutralization

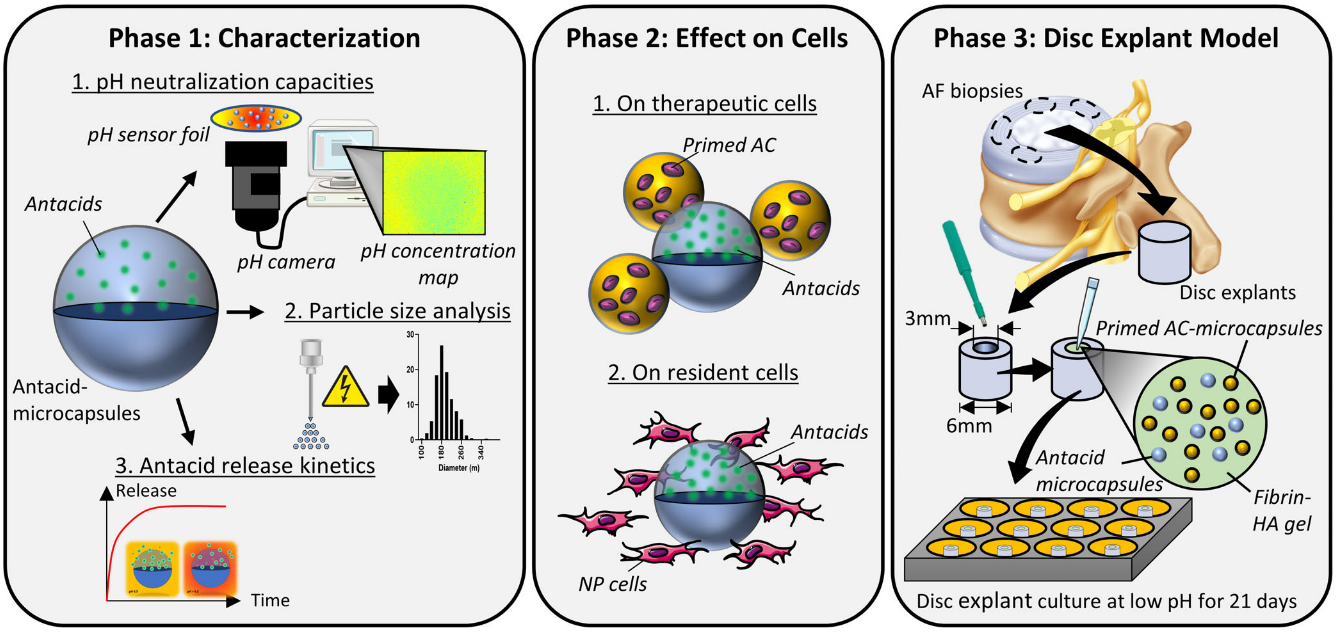

FIGURE 1 Experimental design. Phase 1 investigated physicochemical parameters of different antacids in terms of local pH change, size distribution, and release kinetics. Phase 2 examined the effect of pH buffering microcapsules on cells (therapeutic cells and resident native cells). In phase 3, the combination of cellular microcapsules and antacid microcapsules was assessed in a bovine disc explant model under physiological degenerative-like conditions.

capacities using a pH sensor foil system (PreSens, Germany). Next the size of sprayed antacid microcapsules ($Mg(OH)_2$ or $CaCO_3$) with various concentrations was analyzed and the release kinetics from microcapsules into the local environment at low pH was investigated. The second phase examined the effect of the developed antacid microcapsules on therapeutic cells (primed AC cells) and resident NP cells in terms of viability and matrix accumulation capacities. Finally, the third phase assessed the combination of cellular microcapsules and antacid capsules in a bovine disc explant model under physiological degenerative conditions.

2.2 | Fabrication of antacid microcapsules

The desired amount of various antacids ($Al(OH)_3$, $Mg(OH)_2$, $CaCO_3$, or HEPES) was mixed with 1% alginate (Pronova UP LVG, FMC NovaMatrix, Norway). For homogeneous distribution of the nanoparticles, the suspension was blended using a homogenizer for 2× 1 min cycles followed by 3× 1 min cycles of ultrasonication. The final solution was diluted using 1% alginate to obtain different concentrations (25–500 mg/mL). For microcapsule fabrication, an electrohydrodynamic (EHD) sprayer was used as described in our previous studies.[20,25,32,33] Briefly, the homogenized alginate-antacid solution was loaded into a syringe and passed through a 30G needle at a flow rate of 50 μL/mL and working distance of 50 mm, with an applied voltage of 10–15 kV to achieve a stable Taylor cone. Microcapsules were collected in a dish containing 100 mM $CaCl_2$ to ionically crosslink the alginate polymer.

2.3 | Preparation of low pH media

Low pH media (pH 6.5) was prepared by adding an appropriate amount of acid to low glucose DMEM (lg-DMEM). Briefly, physiological levels of lactic acid (4 mM), typical of those found in the IVD,[1] were added to the media and pH levels were adjusted by adding 3M hydrochloric acid (10 μL/mL). The pH-adjusted media was incubated overnight in a humidified incubator (5% CO_2) to allow buffer equilibrium (CO_2-dependent). The desired pH values were obtained after equilibration and were maintained for up to 72 h.

2.4 | pH mapping and measurements

The pH concentration maps were generated using a USB pH detector unit—microscope device and corresponding software (VisiSens; PreSens GmbH, Regensburg, Germany). Briefly, a circular section measuring 8 mm in diameter was cut from a pH sensor foil while ensuring minimal exposure to light (Product code SF-HP5R, PreSens GmbH, Regensburg, Germany). The circular sensor foil was carefully attached to the bottom of a standard cell culture dish using a silicone glue. The foil was calibrated using a six-point calibration following the manufacturer's instructions. For the experiment, antacid microcapsules within a fibrin (50 mg/mL)-hyaluronic acid (HA) (5 mg/mL) hydrogel was placed on the surface.[31] The construct was cultured in low pH media (pH 6.5) and images were taken from below using a camera-based detector unit (DU02, VisiSens; PreSens GmbH, Regensburg, Germany) at various time points to assess local pH change.

Control wells with known pH levels (7.1 and 6.5) were used to ensure stability of the pH over the time course investigated (72 h). The output file generated by the VisiSens™ AnalytiCal 2 Software (PreSens GmbH, Regensburg, Germany) was analyzed using a custom written MATLAB® code (MathWorks®, Version R2017a, Massachusetts, US). Briefly, every pixel within the produced image file represents a pH value derived from the calibration image, enabling the creation of a pH map across the sensor foil. For explant cultures, pH levels were measured using fiber-optical fluorescent microsensors (PreSens, Regensburg, Germany).

2.5 | Size analysis

For size analysis, antacid microcapsules ($n \sim$350–1000) of each group were imaged using light microscopy, and microcapsule diameters were determined using image analysis software (ImageJ, National Institutes of Health, and Bethesda, Maryland).

2.6 | Antacid salt release kinetics

The amount of calcium and magnesium retained in microcapsules and released into the media was quantified using the Sentinel Calcium and Magnesium Liquid (Alpha Laboratories Ltd., UK) assay kits in accordance with the manufacturer's instructions. At specific time-points in culture, antacid microcapsules were dissolved in 1 M HCl solution for 1 h under constant rotation. Media samples were also analyzed directly without 1 M HCl treatment.

2.7 | Isolation and expansion of primary cells

All animal tissue used in this work was obtained from a local abattoir and did not require ethical approval. IVDs were harvested from the lumbar region of the spine of porcine donors (3–4 months, 20–30 kg) within 3 h. Under aseptic conditions, IVDs were carefully exposed and the gelatinous NP tissue removed from the central section of the disc.[34] To confirm the absence of bacterial growth, dissected tissue was cultured overnight at 37°C, 5% CO_2 in a humidified atmosphere in serum-free low-glucose Dulbecco's Modified Eagles Medium (lg-DMEM, 1 g/L D-glucose) supplemented with 100 U/mL penicillin, 100 μg/mL streptomycin. NP tissue was enzymatically digested in 2.5 mg/mL pronase solution for 1 h followed by 2 h in 0.5 mg/mL collagenase solution at 37°C under constant rotation. The digest was subjected to physical agitation cycles at the start and every 30 min thereafter using a gentlemacs tissue dissociator (Miltenyi Biotech). Digested tissue/cell suspension was passed through a 100-μm cell strainer to remove tissue debris followed by 70 and 40 μm cell strainers to separate notochordal cells from the desired NP cells as previously described.[35] Cells were then washed three times by repeated centrifugation at 650 g for 5 min. NP cells were cultured to confluence in T-75 flasks with lg-DMEM, supplemented with 10% fetal bovine serum (FBS), 100 U/mL penicillin, 100 μg/mL streptomycin, 0.25 μg/mL amphotericin B (AmpB), and 5 ng/mL FGF-2 (PeproTech, UK) at 37°C in a humidified atmosphere with 5% CO_2, and expanded to passage 2 (P2) with medium exchanges performed every 3 days.

Juvenile porcine ACs were isolated from cartilage of the knee joint. Tissue was washed with phosphate buffered saline (PBS) and finely minced. For cell isolation, minced tissue was digested with concentrations of 3000 U/mL collagenase type II (Gibco, Ireland) for ~2.5 h under constant rotation at 37°C in serum-free hg-DMEM, (4.5 mg/mL D Glucose, 200 mM L-Glutamine;) containing antibiotic/antimycotic (100 U/mL penicillin, 100 mg/mL streptomycin) (all Gibco, Invitrogen, Ireland) and AmpB (0.25 μg/mL, Sigma–Aldrich). The digest was subjected to physical agitation cycles at the start and every 30 min thereafter using a gentlemacs tissue dissociator (Miltenyi Biotech, UK).[36] The digested tissue/cell suspension was passed through a 100-μm cell strainer to remove tissue debris and washed three times by repeated centrifugation at 650 g for 5 min. Cell viability was determined with a hemocytometer and trypan blue exclusion. Cells were seeded at an initial density of 5×10^3 cells/cm^2 in media consisting of lg-DMEM (1 mg/mL D-Glucose, Sigma) supplemented with 10% FBS, penicillin (100 U/mL)-streptomycin (100 μg/mL) (all GIBCO, Invitrogen, Ireland), and AmpB (0.25 μg/mL, Sigma–Aldrich, Arklow, Ireland) at 37°C and 5% CO_2. Cells were subcultured at a seeding density of 5×10^3 cells/cm^2 and cultured until passage 1 (~14 days).

2.8 | Cellular microencapsulation

ACs were trypsinized and resuspended in media and combined with sterile 2% alginate solution (Pronova UP LVG, FMC NovaMatrix, Norway) at a 1:1 ratio to yield a final alginate concentration of 1% and a seeding density of 10×10^6 cells/mL. The alginate/cell solution was electrosprayed using an EHD sprayer,[20,25,32,33] with constant processing parameters (30G needle, 10–15 kV applied voltage, 100 μL/mL flow rate, 50 mm working distance). After ionically crosslinking for 5 min inside a 100 mM $CaCl_2$ bath (pH 7.2), microcapsules were rinsed thoroughly with PBS before resuspension in the appropriate medium for culture.

2.9 | In vitro priming of AC microcapsules

AC-containing microcapsules were resuspended in media post-fabrication using a ratio of 25 μL microcapsules per 1 mL of media and primed for 14 days in TGF-β3 (10 ng/mL). Culture media consisted of lg-DMEM supplemented with penicillin (100 U/mL)-streptomycin (100 μg/mL) (GIBCO, Invitrogen, Dublin, Ireland), 0.25 μg/mL AmpB, 40 μg/mL L-proline, 100 nM dexamethasone, 50 μg/mL L-ascorbic acid 2-phosphate, 4.7 μg/mL linoleic acid (all Sigma–Aldrich, Ireland), and 10 ng/mL TGF-β3 (PeproTech, UK). Microcapsules were cultured at 37°C and low oxygen (5% O_2)

conditions for 14 days under constant agitation. Half media exchanges were performed twice weekly.

2.10 | In vitro culture of AC microcapsules and NP cells with antacids

After the priming regime, AC cellular microcapsules and antacid microcapsules were mixed into a fibrin hydrogel (100 mg/mL) and cultured for 24 h for cytotoxicity ($n = 4$ per group). NP cells were directly encapsulated into fibrin hydrogels (4×10^6 cells/mL) in combination with antacid capsules for 24 h to evaluate any cytotoxicity effects ($n = 4$ per group).

2.11 | Assessment of cell viability

Cell viability was assessed using the LIVE/DEAD® viability/cytotoxicity assay kit (Invitrogen, Ireland). Constructs were removed from culture and incubated in phenol free DMEM media containing 2 μM calcein AM and 4 μM ethidium homodimer-1 (EthD-1) (both from Cambridge Bioscience, UK) for 1 hour at 37°C. Following incubation, constructs were imaged with a Leica SP8 scanning confocal microscope at 515 and 615 nm channels and analyzed using Leica Application Suite X (LAS X) software. Cell viability was determined by counting calcein AM positive cells (live) and EthD-1 positive cells (dead) followed by calculation of the percentage (%) of viable cells relative to the total cell population.

2.12 | Disc explant isolation and culture

Skeletally mature bovine tails were obtained from a local abattoir. Discs were isolated with a custom-made guillotine and two parallel blades separated by a distance of 4.5 mm. From each obtained 'disc slab', three to five 6 mm biopsies were taken from the AF-region. AF-cylinders (6 mm) were cored using a 3-mm biopsy punch to generate an annular disc explant, which was inserted into a 3D printed cage to provide confinement and prevent swelling of the tissue. Briefly, cages were 3D printed with a Formlabs 2 printer and dental resin SG V1 (Formlabs, UK). After printing, cages were washed in isopropanol to remove excess resin and cured for 1 hour at 60°C under ultraviolet (UV) light. Subsequently, cages underwent air drying and UV light exposure for surface sterilization prior to use. Based on results acquired during in vitro experiments, the 500 mg/mL $CaCO_3$ group was found to be superior in terms of long-term buffering capacities and cell survival compared with all other experimental groups. Therefore, two groups were compared in an IVD explant model: primed AC without $CaCO_3$ microcapsules ($-CaCO_3$, control) and primed AC with 500 mg/mL $CaCO_3$ microcapsules ($+CaCO_3$) ($n = 5$ for each group, 3 for biochemical analysis and 2 for viability and histological assessment). Briefly, both empty ($-CaCO_3$, control) and $+CaCO_3$ (500 mg/mL) containing alginate microcapsules were prepared; 25 μL of a fibrin (100 mg/mL)-HA (5 mg/mL) blend containing blank or $+CaCO_3$ (500 mg/mL) alginate microcapsules and cellular microcapsules were combined and pipetted into the 3 mm core of disc explants (Figure 1, "Phase 3"). Constructs were cultured in low pH (pH 6.5), high osmolarity (~450 mOsm, adjusted using 150 mM sucrose), chemically defined medium containing lg-DMEM supplemented with 1 mg/mL Primocin (Invivogen, France), 5% FBS (GIBCO, Invitrogen, Dublin, Ireland), 100 KIU/mL aprotinin solution (Nordic Pharma, Sweden), 0.25 μg/mL AmpB, 1.5 mg/mL BSA, 1× ITS, 40 μg/mL L-proline, 100 nM dexamethasone, 50 μg/mL L-ascorbic acid 2-phosphate, and 4.7 μg/mL linoleic acid (all Sigma–Aldrich, Ireland). The total culture period was 21 days at 37°C in physioxic (5% oxygen) conditions, with medium exchanges performed twice weekly.

2.13 | Quantitative biochemical analysis

Three samples of each group were separated (AF ring from hydrogel-core) and both parts digested separately using papain (125 μg/mL) in 0.1-M sodium acetate, 5 mM L-cysteine HCl, 0.05 M EDTA, and sodium citrate (55 mM) (Sigma–Aldrich, Ireland) at 60°C under constant agitation for 18 h followed by an additional incubation with 1-M sodium citrate under constant rotation for 1 h to disrupt the alginate-calcium crosslinks. DNA content of each sample was quantified using the Hoechst Bisbenzimide 33258 dye assay, with a calf thymus DNA standard and expressed in terms of the total amount of DNA (ng) per sample. Proteoglycan content was estimated by quantifying the amount of sGAG in constructs using the dimethylmethylene blue dye-binding assay (DMMB Blyscan, Biocolor Ltd., Northern Ireland, UK), with a chondroitin sulfate standard and expressed as total amount of sGAG measured (μg). Total collagen content was determined for each sample (μg) by measuring the hydroxyproline content. Samples were hydrolyzed at 110°C for 18 h in concentrated HCl (38%) and assayed using a chloramine-T assay[37] and a hydroxyproline-to-collagen ratio of 1:7.69.[38]

2.14 | Histological Analysis

Two samples of each group were fixed in 4% paraformaldehyde (PFA) overnight at 4°C, followed by repeated washings in PBS. Fixed samples were dehydrated in a graded series of ethanol (70% to 100%), embedded in paraffin wax, sectioned at 6 μm, and affixed to microscope slides. Sections were stained with 1% alcian blue 8GX in 0.1 M HCL (alcian blue/aldehyde fuchsin for alginate-based samples) to assess sGAG content and picrosirius red to assess collagen distribution (all from Sigma–Aldrich, Ireland).

2.15 | Statistical analysis

Statistical analyses were performed using GraphPad Prism (version 10.1.1) software with three to four samples analyzed for each experimental group. One-way ANOVA or two-way ANOVA was used for the analysis of variance where appropriate, with Tukey post-tests to compare between groups. The results are displayed as mean ± standard deviation (SD) and significance was accepted at a level of $p < .05$.

3 | RESULTS

3.1 | Antacid microcapsules can increase the local pH within an acidic environment

Different antacids, namely $Mg(OH)_2$, $CaCO_3$, the zwitterion HEPES, and $Al(OH)_3$ at a concentration of 50 mg/mL were compared in terms of buffering capacities when exposed to a low pH environment (pH 6.5) (Figure 2). Results revealed no discernible differences in pH concentration maps between HEPES, $Al(OH)_3$, and the negative control group (pH 6.5 without pH buffering). In contrast, both $Mg(OH)_2$ and $CaCO_3$ increased the pH in the center of the construct to 7.5 and 7.0, respectively (Figure 2A). Comparing pH as a function of distance along the *x*-axis of each construct, it is clear that the main effect of the buffering microcapsules occurs in the center with decreasing pH values toward the periphery (Figure 2B). Comparing the acidity change over time of each group, it is evident that $Mg(OH)_2$ and $CaCO_3$ have the highest pH neutralization capacities. However, $Mg(OH)_2$ was found to increase the pH level to a very basic level (pH 8.47 ± 0.58) within the first 8 h before plateauing toward neutral levels, which may be detrimental for cell viability (Figure 2C). $CaCO_3$ was capable of increasing the local pH to a neutral level for the duration of 72 h (Figure 2C). The desired pH values were obtained after equilibration and were maintained for up to 72 h. Figure 2C also shows the stability of the positive (pH 7.4) and negative (pH 6.5) control wells over the course of 72 h.

3.2 | Increasing antacid concentration increases local pH levels

Based on the previous results (testing different pH buffering agents), $Mg(OH)_2$ and $CaCO_3$ were taken forward to investigate the effect of salt concentration. The temporal effect of $Mg(OH)_2$ and $CaCO_3$ on the local environment within the construct and the surrounding media was evaluated for different initial concentrations (25, 50, 100, 250, and 500 mg/mL) (Figure 3). $Mg(OH)_2$ was observed to alter the pH of the acidic environment to a larger extent depending on the initial salt concentration (Figure 3A). At the highest concentration (500 mg/mL), the local pH of the construct was found to exceed the range of the measuring limits (pH >10) and the pH of the media plateaued at pH 7.9 after 24 h (Figure 3A,B). The local pH of the constructs showed an initial peak within the first 5 h after acidic exposure but decreased toward a neutral pH over time (Figure 3A solid line). Also, the media pH increased over time and reached values between 6.8 and 7.5 after 3 days depending on the initial $Mg(OH)_2$ concentration (Figure 3A). In contrast, changing the concentration of $CaCO_3$ did not exert such large variations on the surrounding pH compared with $Mg(OH)_2$ (Figure 3C,D). Similar to $Mg(OH)_2$, the initial peak occurred within the first 5 h of low pH exposure (Figure 3C), but never exceeded levels above pH 8. The concentration of 500 mg/mL appeared to equilibrate at a neutral pH of 7 locally as well as within the culture media. The lowest concentration (25 mg/mL of $CaCO_3$)

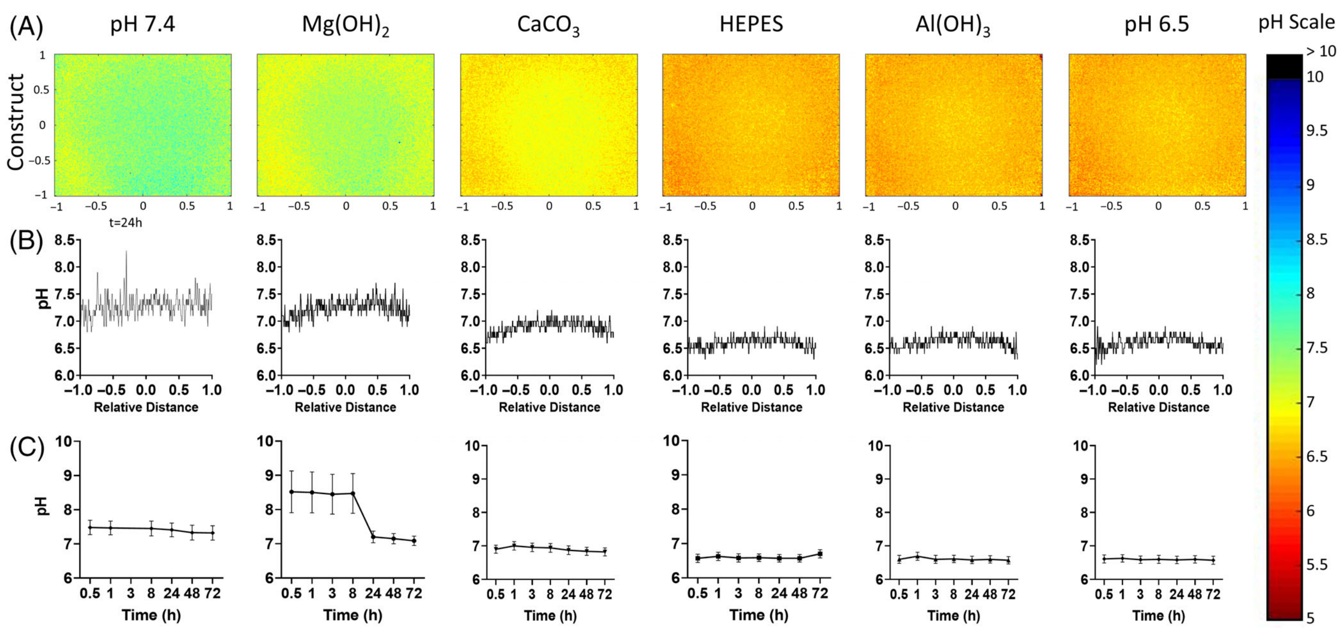

FIGURE 2 Local pH mapping of 50 mg/mL $Mg(OH)_2$, $CaCO_3$, HEPES, and $Al(OH)_3$ microcapsules exposed to low pH media in comparison to controls with constant pH media (7.4 representing positive control and pH 6.5 representing negative control). (A) pH concentration maps at 24 h. (B) pH profile in the x direction after 24 h, and (C) change in local pH evaluated over 72 h. Data shown from one representative sample from a total of $n = 3$ samples evaluated.

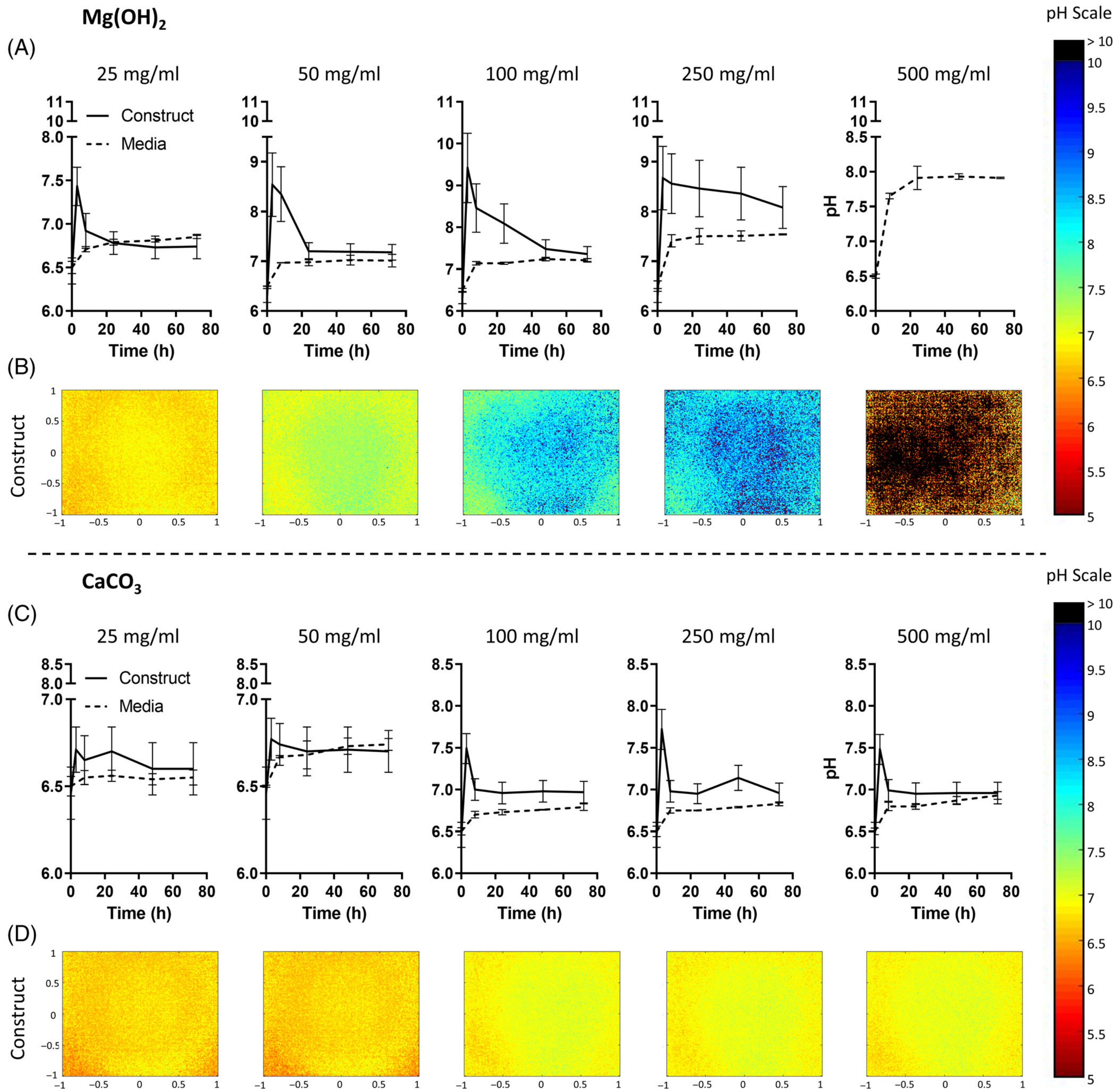

FIGURE 3 Buffering capacity of different concentrations (25–500 mg/mL) of $Mg(OH)_2$ and $CaCO_3$. (A) Temporal effect of $Mg(OH)_2$ on pH level within the hydrogel construct (solid line) and culture media (dashed line). (B) pH concentration map showing local pH distribution for $Mg(OH)_2$ at 24 h. (C) Temporal effect of $CaCO_3$ on pH level within the hydrogel construct (solid line) and culture media (dashed line). (D) pH concentration map showing local pH distribution for $CaCO_3$ at 24 h. Data shown from one representative sample from a total of $n = 3$ samples evaluated from each group.

did not exert any significant effect on pH levels in either the construct or surrounding media (Figure 3C).

3.3 | $Mg(OH)_2$ and $CaCO_3$ microcapsule size and release kinetics

After investigating different concentrations of $Mg(OH)_2$ and $CaCO_3$ in terms of pH neutralization limits, the highest $Mg(OH)_2$ group (500 mg/mL) was excluded as it exceeded the upper pH limit, while the lowest $Mg(OH)_2$ concentration (25 mg/mL) did not exhibit a sustained neutralization effect after 24 h and was therefore omitted. The lower concentrations of $CaCO_3$ (25 and 50 mg/mL) were also excluded as they did not demonstrate a noticeable impact on pH neutralization. Further characterization of the concentrations 50, 100 and 250 mg/mL of $Mg(OH)_2$ and 100, 250 and 500 mg/mL of $CaCO_3$ in terms of microcapsule size and release kinetics was performed. As seen in Figure 4A, $CaCO_3$ produced larger microcapsules (303.1

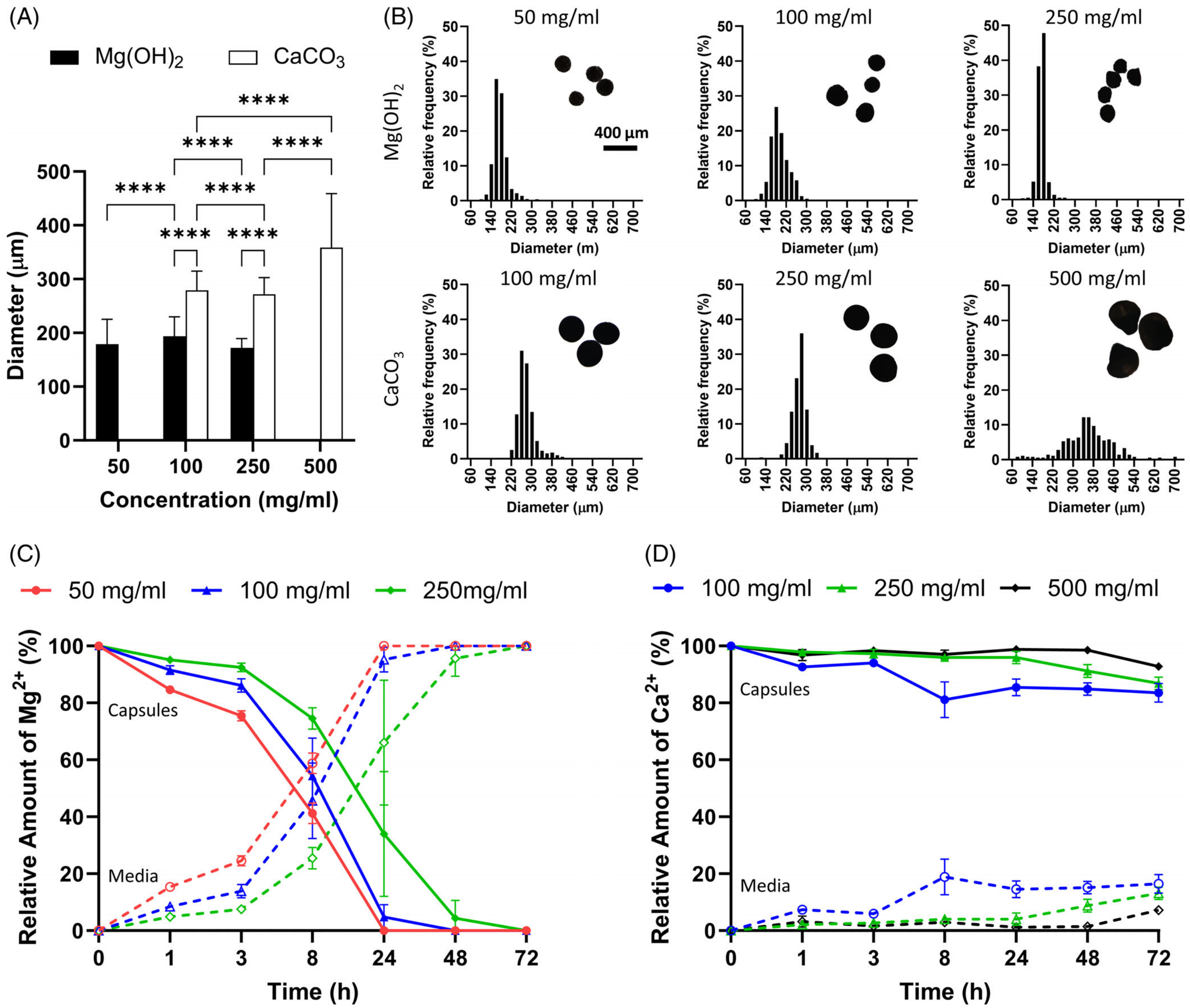

FIGURE 4 Characterization of microcapsules containing different initial concentrations, 50, 100, and 250 mg/mL of $Mg(OH)_2$ and 100, 250, and 500 mg/mL of $CaCO_3$. (A) Average diameter of $Mg(OH)_2$ and $CaCO_3$ microcapsules, **** indicates significant difference ($p < .0001$). (B) Size distribution of $Mg(OH)_2$ (top row) and $CaCO_3$ microcapsules (bottom row) at different concentrations. (C) Relative amount of Mg^{2+} release (%) over 72 h from microcapsules (solid line) into media (dashed line) for different initial concentrations. (D) Relative amount of Ca^{2+} release (%) over 72 h from microcapsules (solid line) into media (dashed line) for different initial concentrations. *n* >350 capsules of each group were analyzed for their size distribution and >100 capsules per sample were analyzed in duplicates for their respective Mg^{2+} or Ca^{2+} release.

± 48.2 μm), whereas $Mg(OH)_2$ exhibited significantly smaller sized microcapsules (181.4 ± 11.1 μm, $p < .0001$). Moreover, comparing size distribution of both antacids at different concentrations reveals a homogeneous microcapsule size for all groups except the highest concentration of $CaCO_3$, which showed a wider range of microcapsule sizes (Figure 4B). Investigating the release of antacids from the microcapsules into the media demonstrated a rapid drop of Mg^{2+} ions inside the microcapsules within the first 24 h, with a concomitant increase in Mg^{2+} concentration in the media (Figure 4C). With respect to Ca^{2+} release from microcapsules into the surrounding media, a decrease of 12.3% ± 4.5% of Ca^{2+} within the microcapsules was observed over the time period investigated (72 h) (Figure 4D). There was no notable distinction in the release kinetics rate for any of the investigated concentrations of $Mg(OH)_2$ and $CaCO_3$.

3.4 | Buffering the local pH using $Mg(OH)_2$ negatively affects NP cells

To evaluate the effect of local pH change in an acidic environment on cell viability, two different aspects were investigated; the impact pH-buffering microcapsules exert on the potential therapeutic-cells (herein termed primed, microencapsulated AC) and on the host cells (NP cells), respectively. Results showed that culturing primed AC microcapsules in the presence of $Mg(OH)_2$ had no significant effect on cell viability with values as high as 92.9% ± 1.8% (Figure 5A,B). In contrast, for NP cells, a significant decrease was observed with increasing concentration of $Mg(OH)_2$ with considerably lower cell viability at concentrations of 250 mg/mL (19.8% ± 12.4%) and 100 mg/mL (31.1% ± 26.5%) compared with AC ($p < .0001$) (Figure 5A,B). In contrast, when culturing cells with $CaCO_3$ loaded microcapsules, a high number (>83%) of viable cells (AC and NP) were observed (Figure 5C,D). Quantification of cell viability revealed levels greater than 80% in all groups with significantly higher cell viability of NP cells compared with AC in all groups (Figure 5D). A significant yet minor reduction in NP cell viability was observed with the highest (500 mg/mL) $CaCO_3$ concentration ($p < .01$) (Figure 5D).

3.5 | $CaCO_3$ significantly increases the pH level within the core of a disc explant cultured under acidic conditions

Buffering capacities were further assessed in a disc explant study, whereby a ring explant from a bovine AF tissue was taken, cored using a 3-mm biopsy punch and filled with a hybrid hydrogel with ($+CaCO_3$) and without ($-CaCO_3$) buffering microcapsules at a concentration of 500 mg/mL. This explant was further cultured inside a 3D printed cage to prevent excessive tissue swelling (Figure 6A). After 21 days in culture under disc-like acidic conditions of pH 6.5, pH values within the core were measured using a fiberoptic pH microsensor (Figure 6B). Results demonstrated a significantly higher pH level within the core when using primed AC cells and $+CaCO_3$ microcapsules in a hybrid gel compared to a control gel without ($-CaCO_3$) microcapsules ($p < .0001$) (Figure 6C).

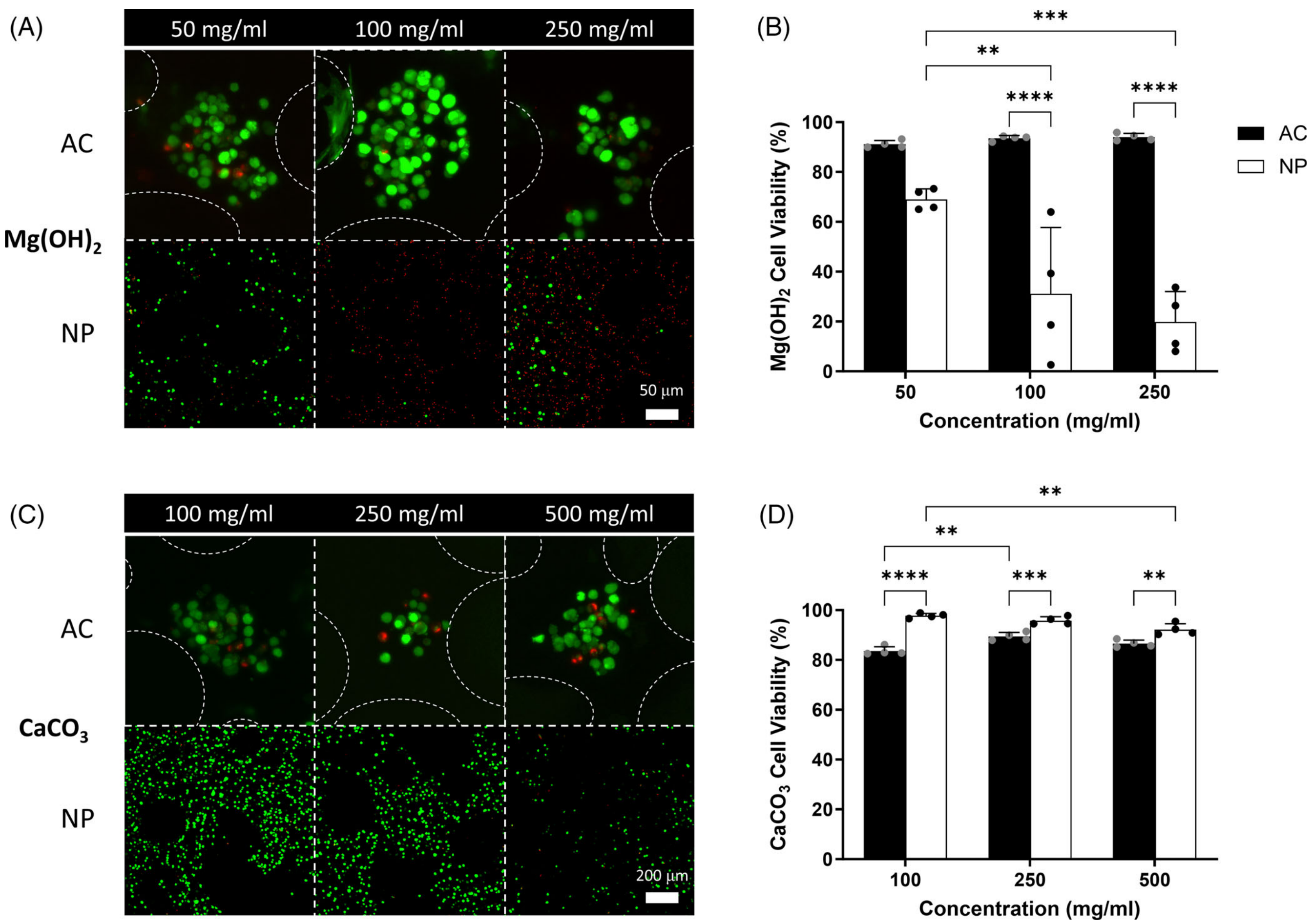

FIGURE 5 Concentration effects of $Mg(OH)_2$ and $CaCO_3$ buffering microcapsules on AC (primed) and NP cells, respectively. (A) Live/Dead assessment of cells after 24 h exposure to media with a pH of 6.5 in the presence of $Mg(OH)_2$ buffering microcapsules. (B) Semi-quantitative image analysis of cell viability when cultured at pH 6.5 with $Mg(OH)_2$ loaded microcapsules at various concentrations (50, 100, and 250 mg/mL). (C) Live/Dead assessment of cells after 24 h exposure to media with a pH of 6.5 in the presence of $CaCO_3$ buffering microcapsules. (D) Semi-quantitative image analysis of cell viability when cultured at pH 6.5 with $CaCO_3$ loaded microcapsules at various concentrations (100, 250, and 500 mg/mL). A sample size of $n = 4$ biological replicates per group were analyzed. **, ***, and **** indicate significant differences between groups ($p < .01$, $p < .001$, and $p < .0001$, respectively). AC, articular chondrocyte; NP, nucleus pulposus.

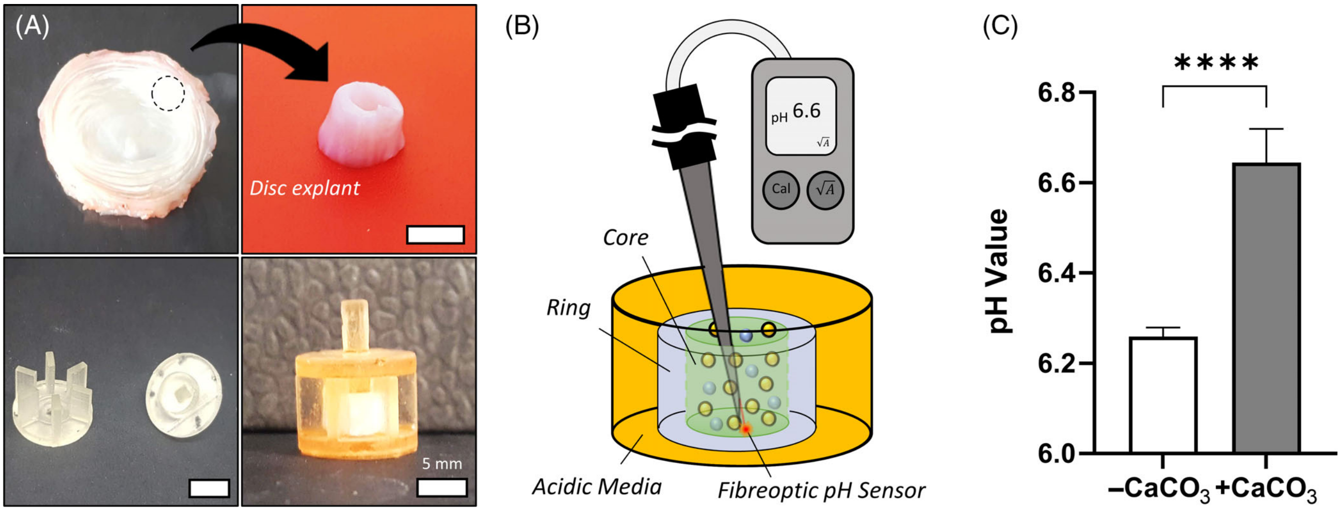

FIGURE 6 The pH measurements within explants after 21 days of acidic culture. (A) Explants were biopsied from bovine discs to create annular rings, which were cultured in 3D printed cages. Scale bar = 5 mm (B) schematic of pH measurement procedure (C) pH values measured within the core of cultured explants with (+$CaCO_3$) and without (−$CaCO_3$) buffering microcapsules. **** indicates significant difference ($p < .0001$). pH was measured in $n = 5$ replicates, with measurements taken in triplicate per sample using a fiber optic pH sensor.

3.6 | $CaCO_3$ buffering curtails DNA loss within the core while preserving DNA content within disc tissue

Within the core gel, DNA levels were reduced relative to day 0 for the −$CaCO_3$ group ($p < .05$), with no significant differences observed for gels containing buffering microcapsules (+$CaCO_3$) at day 21 (Figure 7A). DNA content appeared to be maintained in the explant tissue for both ±$CaCO_3$ groups (Figure 7B). Densely packed viable AC microcapsules were observed within the core of both ±$CaCO_3$ groups, indicated with green calcein staining (Figure 7C). Semi-quantitative analysis of cell viability within the core was found to be high for both groups, with higher viability (96.2% ± 1.7%) in the −$CaCO_3$ group relative to the +$CaCO_3$ (89.3% ± 3.5%) (Figure 7 D).

3.7 | $CaCO_3$ buffering enhances core sGAG levels and curtails depletion within disc tissue

To evaluate the change in sGAG levels within the hybrid gel (core) and the disc tissue (ring), the two compartments were separated and analyzed individually (Figure 8). Gels containing buffering microcapsules (+$CaCO_3$) resulted in higher levels of sGAG at day 21 (Figure 8A). Similar findings were observed for the explant tissue, with $CaCO_3$ curtailing the loss of sGAG which was significantly lower in −$CaCO_3$ group compared to day 0 (Figure 8B). Deep purple-stained primed AC microcapsules were visible within the gel core for both ±$CaCO_3$ explant groups (Figure 8C).

3.8 | $CaCO_3$ buffering maintains collagen content in explant culture

In terms of total collagen, no significant differences were observed for explants cultured with (+) or without (−) $CaCO_3$ microcapsules for either the core (Figure 9A) or the ring (Figure 9B) domains. No appreciable differences in picrosirius red collagen staining were observed between the groups, which correlated with the biochemical quantification (Figure 9C).

4 | DISCUSSION

The acidic microenvironment of the IVD plays a critical role in the imbalance of matrix anabolism and catabolism, which is believed to be a primary reason for the degeneration of the NP and subsequent low back pain.[15,39] The overall aim of this study was to develop and characterize pH buffering microcapsules to alter the low pH disc microenvironment and support host cells to either maintain or even rejuvenate disc tissue composition. Finally, these microcapsules were evaluated in vitro and ex vivo to verify their potential when subjected to native disc-like microenvironmental conditions.

During the first phase of this study, different salts and buffering agents were investigated in terms of their pH neutralization capacities, which showed a limited effect of HEPES and $Al(OH)_3$ compared with $Mg(OH)_2$ and $CaCO_3$. HEPES is capable of maintaining the pH within a neutral range (pH 6.8–8.2), which is typically desired in standard cell culture media. A pH of 6.5 was used to represent degenerative disc conditions, which appeared beyond the range to be adequately affected by HEPES. The weak base $Al(OH)_3$ is mostly insoluble within a pH range of pH 6–pH 8 and thus resulted in poor neutralization capacities. In contrast, $Mg(OH)_2$ and $CaCO_3$ were found to raise the pH, even to an alkaline range in the case of $Mg(OH)_2$. $Mg(OH)_2$ is a strong base, which dissociates into $Mg^{2+}_{(aq)}$ and $2OH^-_{(aq)}$ under acidic conditions. The increase of OH^- ions within the surrounding solution creates an imbalance between H_3O^+ and OH^- causing a shift toward an alkaline pH, which is accelerated due to the high diffusion coefficient of OH^- (5.27×10^{-5} cm^2/s,[40]). $CaCO_3$ is a mostly insoluble weak base, which dissociates into $Ca^{2+}_{(aq)}$,

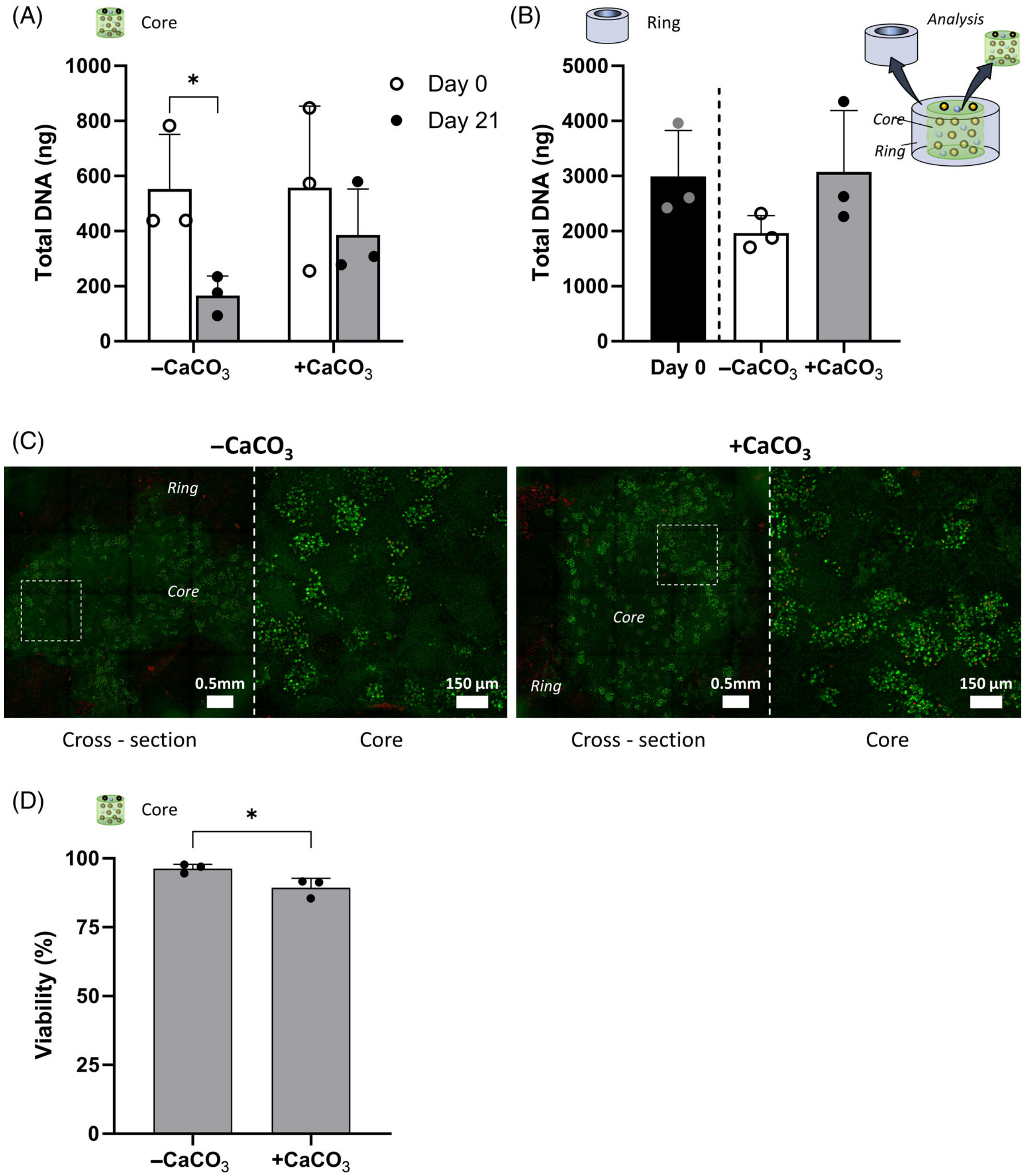

FIGURE 7 DNA content and cell viability of cultured bovine annular ring explants containing a gel core with encapsulated primed articular chondrocyte cells with (+) and without (−) $CaCO_3$ buffering microcapsules after 21 days. (A) Total DNA (ng) content within the gel core. (B) Total DNA content (ng) of the explant ring compared to day 0. * indicates significant difference ($p < .05$). (C) Confocal images of viable (green) and dead (red) cells. Sectioning was performed in the transverse direction. (D) Semi-quantitative image analysis of cell viability within the core region at day 21. A sample size of $n = 3$ was analyzed per group.

$HCO_3^-{}_{(aq)}$, and $H_2O.CO_{2(aq)}$ within an acidic solution. The diffusion coefficient of HCO_3^- is 4.4 times lower than that of OH^- explaining the slower increase in pH using $CaCO_3$ compared with $Mg(OH)_2$. This neutralization capacity is mostly dependent on the local acidity, and not significantly influenced by other microenvironmental factors of the disc such as CO_2, O_2, or glucose levels. However, cell culture media contains sodium bicarbonate, which is commonly used to maintain a neutral pH under 5% CO_2 conditions, which may increase the rate of neutralization while both neutralizers react with the free H^+ ions. The media used was supplemented with acids capable of maintaining a low pH of 6.5 for at least 72 h, suggesting that the bicarbonate from the media alone is not sufficient to increase the pH level. Hence, the buffering observed in this study is most likely attributed to the antacid used.

Microcapsule size and associated release kinetics also affect neutralization capacities of antacids. Evaluating different concentrations

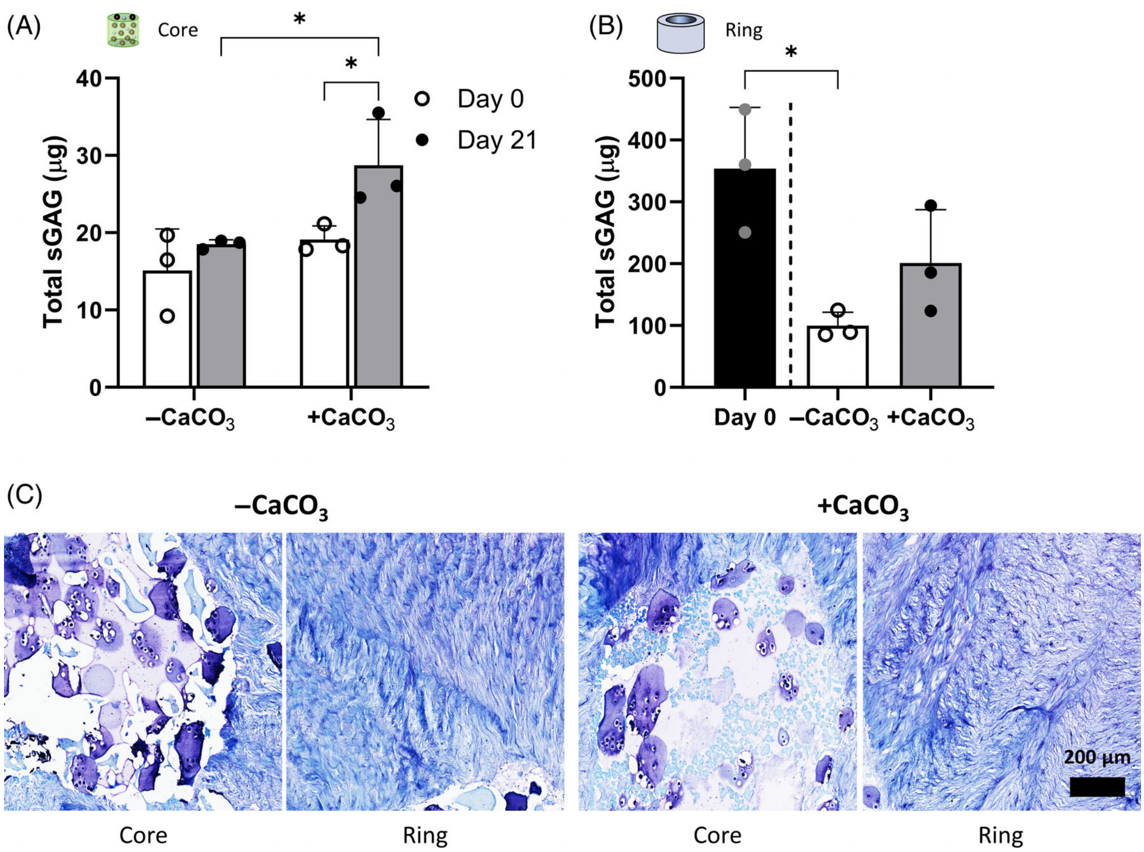

FIGURE 8 sGAG accumulation of cultured bovine annular ring explants containing a gel core with encapsulated primed AC cells with (+) and without (−) $CaCO_3$ buffering microcapsules after 21 days. (A) Total sGAG (µg) within the gel core. (B) Total sGAG (µg) of the explant ring relative to day 0. * indicates significant difference ($p < .05$). (C) Alcian blue/aldehyde fuchsin staining indicating sGAG within core and ring regions. Sectioning was performed in the transverse direction. A sample size of $n = 3$ was analyzed per group.

of $Mg(OH)_2$ and $CaCO_3$ entrapped in alginate microcapsules revealed significantly larger microcapsules using $CaCO_3$ with the largest diameter observed when fabricating 500 mg/mL microcapsules (358.6 ± 100.3 µm). There are two possible reasons for this; the $CaCO_3$ nanoparticles used were two to three times bigger than those for $Mg(OH)_2$ microcapsules, which can influence the viscosity of alginate-antacid slurries. Second, $CaCO_3$ can induce partial crosslinking of alginate,[41] which also increases the viscosity of the solution. Both influence the rheologic properties and hence EHD spraying properties.[32]

With respect to release kinetics, a faster diffusion of Mg^{2+} ions from the microcapsules into the media was demonstrated compared to Ca^{2+} ions for all concentrations investigated. Both antacids are considered insoluble in water. However, as pH decreases, solubility increases with a 3-fold higher solubility of $CaCO_3$ at pH 6.0 compared with a neutral pH.[42] However, Ca^{2+} ions have a higher affinity toward alginate compared with Mg^{2+} ions, retarding their rapid release from the alginate network while Mg^{2+} is more readily released into the media. Mg^{2+} ions were found to be fully released within 72 h, whereas 80% of Ca^{2+} ions remained within the microcapsules with a predicted complete release after several weeks. While alginate relies on calcium crosslinking to form a stable hydrogel, it is unlikely that the additional Ca^{2+} contributed by the $CaCO_3$ had any noticeable impact on the alginate stiffness as ionic crosslinking sites are well saturated due to the reaction with $CaCl_2$ as part of the crosslinking step. There are several alternative natural (fibrin, collagen, chitosan, and pectin) and synthetic (PLGA, PCL) biopolymers compatible with the electrohydrodynamic process[33] that could be used for $CaCO_3$ encapsulation, which provides ample opportunity for optimization of microcapsule size and release kinetics.

However, extracellular calcium concentrations can affect biological processes. Previous work has shown that levels above 20 mM can induce apoptosis in osteoclasts,[43] while levels of 0.5 mM can activate calcium signaling receptors in cartilage endplate cells, leading to suppressed matrix deposition.[44] In this study, within a 72-h timeframe, approximately 0.08 mM of calcium was released into the media for the $CaCO_3$ (500 mg/mL) loaded microcapsules, which is also below the normal range of calcium serum levels (1.9–2.5 mM). This concentration falls below toxic levels and is therefore unlikely to induce apoptosis or other forms of cellular damage. However, whether accumulated levels of calcium within the disc itself will exceed a critical threshold and negatively impact cells warrants further investigation. The mild buffering behavior and the slower release kinetics of $CaCO_3$ could be considered major advantages compared to $Mg(OH)_2$.

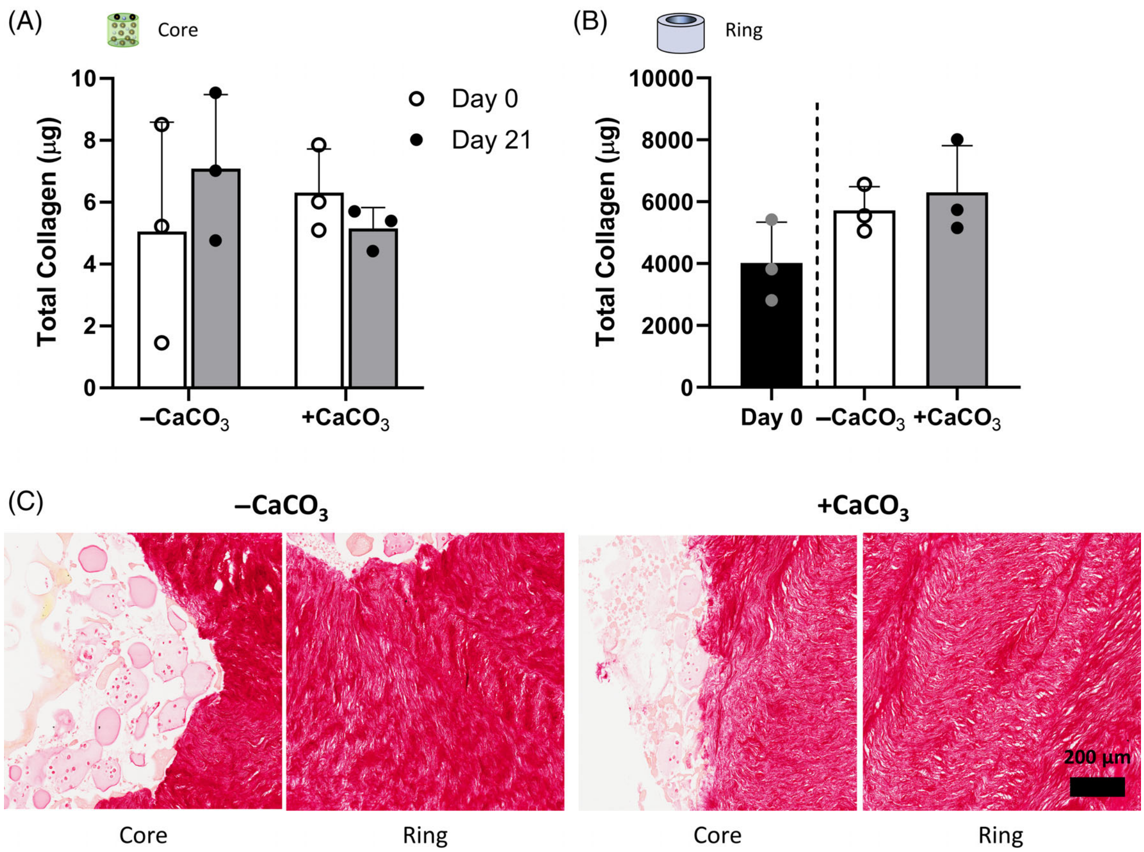

FIGURE 9 Collagen accumulation of cultured bovine annular ring explants containing a gel core with encapsulated primed AC cells with (+) and without (−) $CaCO_3$ buffering microcapsules after 21 days. (A) Total collagen (µg) within the gel core. (B) Total collagen (µg) of the explant ring relative to day 0. (C) Picrosirius red staining indicating collagen within core and ring regions. Sectioning was performed in the transverse direction. A sample size of $n = 3$ was analyzed per group.

After excluding HEPES and $Al(OH)_3$ from further investigations due to poor neutralization capacities, the effect of $Mg(OH)_2$ and $CaCO_3$ on cell bioactivity was investigated. Examining cell viability of primed AC, no difference was observed between groups. A powerful resilience of primed AC when exposed to low pH conditions has previously been demonstrated in our laboratory,[22] which may be equally resilient when exposed to a basic environment created by $Mg(OH)_2$. NP cells, on the other hand exhibited significant cell death within 24 h when cultured with $Mg(OH)_2$ microcapsules which was amplified with increasing concentration. This was found to occur predominantly in the peripheral region around antacid microcapsules, suggesting that the basic pH around the microcapsule boundaries is detrimental for these cells. Extreme extracellular pH conditions have previously been reported to increase the expression of calcium-sensing receptors (CaSR) in some cells,[45] through binding of Ca^{2+} and Mg^{2+} ions, thereby activating intracellular pathways involved in apoptosis, cell proliferation, survival, and cell maturation.[46,47] Increased activation of this receptor due to basic pH and increased Mg^{2+} levels may overstimulate NP cells resulting in cell death.

In phase 3 of this study, the potential of a hybrid hydrogel containing $CaCO_3$ microcapsules and microcapsules containing primed AC within a fibrin-HA bulking gel was explored using a disc explant model. In the first instance, the neutralization capacities of $CaCO_3$ observed in vitro were validated, demonstrating significantly higher pH levels within the core gel of the explants. After separating the core gel from the disc explant ring for individual analysis, higher DNA levels were found in the gel containing $CaCO_3$ microcapsules emphasizing the protective effects of $CaCO_3$ against the acidic environment. DNA levels within the disc tissue ring of $CaCO_3$ group did not increase compared with day 0 levels, however, levels could be maintained over 21 days of low pH culture most likely due to the pH elevating properties of $CaCO_3$.

Higher levels of sGAG were observed in gel cores containing $+CaCO_3$ buffering microcapsules demonstrating the positive effect of maintaining a neutral pH. In contrast, no significant changes were observed between day 0 and day 21 for the $-CaCO_3$ group which is consistent with previous findings, where pericellular sGAG levels were maintained in acidic environments after priming, potentially due to a balance between TIMP expression during priming followed by MMP release during low pH exposure.[48–50] Within the disc ring, diminished levels of sGAG after 21 days in simulated degenerative disc-like conditions (i.e., low pH, low glucose, and high osmolarity) were demonstrated for both groups, with the $-CaCO_3$ group being significantly lower than day 0 levels. sGAG is readily eluted from disc tissue, even in high osmolarity conditions. Previous work by van Dijk et al. examined sucrose and polyethylene glycol to match osmotic pressure present in native disc tissue. They revealed increased osmolarity, tissue swelling, and loss of proteoglycans (PGs) from the tissue when using sucrose,[51] which correlates with findings observed in this study. This concomitant depletion of PGs from the disc tissue may be masking any beneficial effect of the $CaCO_3$ microcapsules on resident disc cells. Nevertheless, higher levels of total sGAG were observed in the $+CaCO_3$ group, which was not significantly different to day 0 and may be due to higher pH levels as reported previously.[14,17,18] Interestingly, this beneficial effect was not observed for collagen content in either the gel core or within the explant ring.

Explant models offer many of the inherent advantages of full organ culture models, such as the preservation of cells within their native tissue structure, cellular composition, and cell–cell arrangements. In this study, an important objective was to be able to segregate the core and annular regions to evaluate the impact of the pH buffering system in a simplified and high-throughput manner. However, it is important to acknowledge that the fibrin core utilized in the explant model differs significantly from native NP tissue, resulting in distinct diffusion kinetics that may affect the effectiveness of the antacid microcapsules. Furthermore, this study utilizes an AF explant model instead of an NP explant model. This alternative AF explant model was chosen due to the natural swelling properties and the loss of proteoglycans from NP tissue typically experienced in an in vitro system, which is driven by insufficient osmotic pressure compared with its native environment.[51] An AF explant model therefore is more appropriate for this type of study. However, some microcapsules may have been lost due to the fibrin-HA hydrogel degradation, increasing the variability in the biochemical measurements. Future studies should consider employing full organ culture or animal models to represent the in vivo scenario more closely. This will further address the limitation of the lack of integrity of the full organ and biomechanical stimulation. The IVD naturally experiences complex biomechanical stimuli including compression, torsion, flexion, and shear in different intensities and frequencies, which have differing effects on cell fate.[52] For instance, dynamic compression loading has been found to enhance nutrient transport, including growth factors such as TGF-β and FGF, which in turn affects NP cells.[53] Moreover, cyclic mechanical loading can induce chondrogenic differentiation of BMSC and enhance ECM deposition.[54] These aspects were not considered in this work but may provide important insights into the matrix repair capacities for NP tissue repair.

5 | CONCLUSION

Overall, this study developed and characterized pH buffering microcapsules that can neutralize the acidic microenvironment that typically exists in degenerative disc disease. Comparing five different pH neutralizing agents, $CaCO_3$ was found to be superior in terms of neutralization capacities, release kinetics, and positive cellular response. Specifically, $CaCO_3$ elevated the acidic pH to neutral levels, which is estimated to be maintained for several weeks based on Ca^{2+} release kinetics. Additionally, $CaCO_3$ was found to be cytocompatible for both AC and NP cell types cultured in low pH conditions in vitro. Using a disc explant model, it was demonstrated that $CaCO_3$ microcapsules were capable of increasing the local pH within the core of a hybrid gel containing microcapsules of $CaCO_3$ and cells. This study underscores the proof-of-concept that pH-neutralizing agents possess the potential to beneficially modify the challenging acidic microenvironment associated with degenerative disc disease. Furthermore, these findings may have implications for addressing the early stages of disc degeneration in conjunction with cell therapies to augment regeneration.

ACKNOWLEDGMENTS

This work was supported by a Science Foundation Ireland: Career Development Award (15/CDA/3476).

CONFLICT OF INTEREST STATEMENT

The authors declare no conflicts of interest.

DATA AVAILABILITY STATEMENT

The data that support the findings of this study are available from the corresponding author upon reasonable request.

ORCID

Conor T. Buckley https://orcid.org/0000-0001-7452-4534

REFERENCES

1. Bartels EM, Fairbank JC, Winlove CP, Urban JP. Oxygen and lactate concentrations measured in vivo in the intervertebral discs of patients with scoliosis and back pain. *Spine (Phila Pa 1976)*. 1998;23(1):1-7. discussion 8.
2. Selard E, Shirazi-Adl A, Urban JP. Finite element study of nutrient diffusion in the human intervertebral disc. *Spine (Phila Pa 1976)*. 2003; 28(17):1945-1953. discussion 1953.
3. Nachemson A. Intradiscal measurements of pH in patients with lumbar rhizopathies. *Acta Orthop Scand*. 1969;40(1):23-42.
4. Bibby SR, Urban JP. Effect of nutrient deprivation on the viability of intervertebral disc cells. *Eur Spine J*. 2004;13(8):695-701.
5. Gruber HE, Johnson TL, Leslie K, et al. Autologous intervertebral disc cell implantation: a model using Psammomys obesus, the sand rat. *Spine (Phila Pa 1976)*. 2002;27(15):1626-1633.
6. Okuma M, Mochida J, Nishimura K, Sakabe K, Seiki K. Reinsertion of stimulated nucleus pulposus cells retards intervertebral disc degeneration: an in vitro and in vivo experimental study. *J Orthop Res*. 2000; 18(6):988-997.
7. Nomura T, Mochida J, Okuma M, Nishimura K, Sakabe K. Nucleus pulposus allograft retards intervertebral disc degeneration. *Clin Orthop Relat Res*. 2001;389:94-101.
8. Richardson SM, Hoyland JA. Stem cell regeneration of degenerated intervertebral discs: current status. *Curr Pain Headache Rep*. 2008; 12(2):83-88.
9. Wu J, Wang D, Ruan D, et al. Prolonged expansion of human nucleus pulposus cells expressing human telomerase reverse transcriptase mediated by lentiviral vector. *J Orthop Res*. 2014;32(1):159-166.
10. Vedicherla S, Buckley CT. In vitro extracellular matrix accumulation of nasal and articular chondrocytes for intervertebral disc repair. *Tissue Cell*. 2017;49(4):503-513.

11. Urits I, Capuco A, Sharma M, et al. Stem cell therapies for treatment of Discogenic low Back pain: a comprehensive review. *Curr Pain Headache Rep*. 2019;23(9):65.
12. Diamant B, Karlsson J, Nachemson A. Correlation between lactate levels and pH in discs of patients with lumbar rhizopathies. *Experientia*. 1968;24(12):1195-1196.
13. Urban JP. The role of the physicochemical environment in determining disc cell behaviour. *Biochem Soc Trans*. 2002;30(Pt 6):858-864.
14. Wuertz K, Godburn K, Iatridis JC. MSC response to pH levels found in degenerating intervertebral discs. *Biochem Biophys Res Commun*. 2009;379(4):824-829.
15. Bibby SRS, Da J, Ripley RM, Urban JPG. Metabolism of the intervertebral disc: effects of low levels of oxygen, glucose, and pH on rates of energy metabolism of bovine nucleus pulposus cells. *Spine*. 2005;30:487-496.
16. Ohshima K, Nakaya T, Inoue AK, Hataya T, Hayashi Y, Shikata E. Production and characteristics of strain common antibodies against a synthetic polypeptide corresponding to the C-terminal region of potato virus Y coat protein. *J Virol Methods*. 1992;40(3):265-273.
17. Razaq S, Wilkins RJ, Urban JP. The effect of extracellular pH on matrix turnover by cells of the bovine nucleus pulposus. *Eur Spine J*. 2003;12(4):341-349.
18. Naqvi SM, Buckley CT. Bone marrow stem cells in response to intervertebral disc-like matrix acidity and oxygen concentration: implications for cell-based regenerative therapy. *Spine (Phila Pa 1976)*. 2016;41(9):743-750.
19. Borrelli C, Buckley CT. Synergistic effects of acidic pH and proinflammatory cytokines IL-1β and TNF-α for cell-based intervertebral disc regeneration. *Appl Sci*. 2020;10(24):9009.
20. Naqvi SM, Gansau J, Buckley CT. Priming and cryopreservation of microencapsulated marrow stromal cells as a strategy for intervertebral disc regeneration. *Biomed Mater*. 2018;13(3):34106.
21. Grunhagen T, Wilde G, Soukane DM, Shirazi-Adl SA, Urban JP. Nutrient supply and intervertebral disc metabolism. *J Bone Joint Surg Am*. 2006;88(Suppl 2):30-35.
22. Gansau J, Buckley CT. Priming as a strategy to overcome detrimental pH effects on cells for intervertebral disc regeneration. *Eur Cell Mater*. 2021;41:153-169.
23. Samuel S, McDonnell EE, Buckley CT. Effects of growth factor combinations TGFβ3, GDF5 and GDF6 on the matrix synthesis of nucleus pulposus and nasoseptal chondrocyte self-assembled microtissues. *Appl Sci*. 2022;12(3):1453.
24. Dashtdar H, Rothan HA, Tay T, et al. A preliminary study comparing the use of allogenic chondrogenic pre-differentiated and undifferentiated mesenchymal stem cells for the repair of full thickness articular cartilage defects in rabbits. *J Orthop Res*. 2011;29(9):1336-1342.
25. Naqvi SM, Gansau J, Gibbons D, Buckley CT. In vitro co-culture and ex vivo organ culture assessment of primed and cryopreserved stromal cell microcapsules for intervertebral disc regeneration. *Eur Cell Mater*. 2019;37:134-152.
26. Sontag SJ. The medical management of reflux esophagitis. Role of antacids and acid inhibition. *Gastroenterol Clin North Am*. 1990;19(3):683-712.
27. Chen S, Zhao D, Li F, Zhuo R-X, Cheng S-X. Co-delivery of genes and drugs with nanostructured calcium carbonate for cancer therapy. *RSC Adv*. 2012;2(5):1820-1826.
28. Shi H, Li L, Zhang L, et al. Designed preparation of polyacrylic acid/calcium carbonate nanoparticles with high doxorubicin payload for liver cancer chemotherapy. *CrstEngComm*. 2015;17(26):4768-4773.
29. Zhao Y, Luo Z, Li M, et al. A preloaded amorphous calcium carbonate/doxorubicin@silica nanoreactor for pH-responsive delivery of an anticancer drug. *Angew Chem Int Ed Engl*. 2015;54(3):919-922.
30. Chen F, Zhang Z, Deng Z, et al. Controlled-release of antacids from biopolymer microgels under simulated gastric conditions: impact of bead dimensions, pore size, and alginate/pectin ratio. *Food Res Int*. 2018;106:745-751.
31. Gansau J, Buckley CT. Incorporation of collagen and hyaluronic acid to enhance the bioactivity of fibrin-based hydrogels for nucleus pulposus regeneration. *J Funct Biomater*. 2018;9(3):43.
32. Gansau J, Kelly L, Buckley CT. Influence of key processing parameters and seeding density effects of microencapsulated chondrocytes fabricated using electrohydrodynamic spraying. *Biofabrication*. 2018;10(3):035011.
33. Naqvi SM, Vedicherla S, Gansau J, McIntyre T, Doherty M, Buckley CT. Living cell factories—electrosprayed microcapsules and microcarriers for minimally invasive delivery. *Adv Mater*. 2016;28(27):5662-5671.
34. Naqvi SM, Buckley CT. Differential response of encapsulated nucleus pulposus and bone marrow stem cells in isolation and coculture in alginate and chitosan hydrogels. *Tissue Eng Part A*. 2015;21(1–2):288-299.
35. Spillekom S, Smolders LA, Grinwis GC, et al. Increased osmolarity and cell clustering preserve canine notochordal cell phenotype in culture. *Tissue Eng Part C Methods*. 2014;20(8):652-662.
36. Vedicherla S, Buckley CT. Rapid chondrocyte isolation for tissue engineering applications: the effect of enzyme concentration and temporal exposure on the matrix forming capacity of nasal derived chondrocytes. *Biomed Res Int*. 2017;2017:2395138.
37. Kafienah W, Sims TJ. Biochemical methods for the analysis of tissue-engineered cartilage. *Methods Mol Biol*. 2004;238:217-230.
38. Ignat'eva NY, Danilov NA, Averkiev SV, Obrezkova MV, Lunin VV, Sobol' EN. Determination of hydroxyproline in tissues and the evaluation of the collagen content of the tissues. *J Anal Chem*. 2007;62(1):51-57.
39. Luoma K, Riihimaki H, Luukkonen R, Raininko R, Viikari-Juntura E, Lamminen A. Low back pain in relation to lumbar disc degeneration. *Spine (Phila Pa 1976)*. 2000;25(4):487-492.
40. Vany'sek P. Ionic conductivity and diffusion at infinite dilution. In: Haynes WM, ed. *CRC Handbook of Chemistry and Physics*. CRC Press, Taylor & Francis Group; 2014.
41. Liu XD, Yu WY, Zhang Y, et al. Characterization of structure and diffusion behaviour of Ca-alginate beads prepared with external or internal calcium sources. *J Microencapsul*. 2002;19(6):775-782.
42. Plummer LN, Busenberg EJG. The solubilities of calcite, aragonite and vaterite in CO_2-H_2O solutions between 0 and 90°C, and an evaluation of the aqueous model for the system $CaCO_3$-CO_2-H_2O. *Geochimica et Cosmochimica Acta*. 1982;46(6):1011-1040.
43. Lorget F, Kamel S, Mentaverri R, et al. High extracellular calcium concentrations directly stimulate osteoclast apoptosis. *Biochem Biophys Res Commun*. 2000;268(3):899-903.
44. Grant MP, Epure LM, Bokhari R, Roughley P, Antoniou J, Mwale F. Human cartilaginous endplate degeneration is induced by calcium and the extracellular calcium-sensing receptor in the intervertebral disc. *Eur Cell Mater*. 2016;32:137-151.
45. Quinn SJ, Bai M, Brown EM. pH sensing by the calcium-sensing receptor. *J Biol Chem*. 2004;279(36):37241-37249.
46. Brennan SC, Conigrave AD. Regulation of cellular signal transduction pathways by the extracellular calcium-sensing receptor. *Curr Pharm Biotechnol*. 2009;10(3):270-281.
47. Zhang C, Zhang T, Zou J, et al. Structural basis for regulation of human calcium-sensing receptor by magnesium ions and an unexpected tryptophan derivative co-agonist. *Sci Adv*. 2016;2(5):e1600241.
48. Leivonen SK, Lazaridis K, Decock J, Chantry A, Edwards DR, Kahari VM. TGF-beta-elicited induction of tissue inhibitor of metalloproteinases (TIMP)-3 expression in fibroblasts involves complex interplay between Smad3, p38alpha, and ERK1/2. *PLoS One*. 2013;8(2):e57474.
49. Gilbert HTJ, Hodson N, Baird P, Richardson SM, Hoyland JA. Acidic pH promotes intervertebral disc degeneration: acid-sensing ion channel −3 as a potential therapeutic target. *Sci Rep*. 2016;6:37360.

50. Han B, Wang HC, Li H, et al. Nucleus pulposus mesenchymal stem cells in acidic conditions mimicking degenerative intervertebral discs give better performance than adipose tissue-derived mesenchymal stem cells. *Cells Tissues Organs*. 2014;199(5–6):342-352.
51. van Dijk B, Potier E, Ito K. Culturing bovine nucleus pulposus explants by balancing medium osmolarity. *Tissue Eng Part C Methods*. 2011; 17(11):1089-1096.
52. Vergroesen PP, Kingma I, Emanuel KS, et al. Mechanics and biology in intervertebral disc degeneration: a vicious circle. *Osteoarthr Cartil*. 2015;23(7):1057-1070.
53. Fearing BV, Hernandez PA, Setton LA, Chahine NO. Mechanotransduction and cell biomechanics of the intervertebral disc. *JOR Spine*. 2018;1(3):e1026.
54. Huang YC, Leung VY, Lu WW, Luk KD. The effects of microenvironment in mesenchymal stem cell-based regeneration of intervertebral disc. *Spine J*. 2013;13(3):352-362.

How to cite this article: Gansau J, McDonnell EE, Buckley CT. Development and characterization of antacid microcapsules to buffer the acidic intervertebral disc microenvironment. *J Biomed Mater Res*. 2024;1-16. doi:10.1002/jbm.a.37755